Electronics using hybrid-molecular and mono-molecular devices

C. Joachim*, J. K. Gimzewski† & A. Aviram‡

* *Centre d'Elaboration de Matériaux et d'Etudes Structurales–Centre National de la Recherche Scientifique, 29 rue J. Marvig, 31055 Toulouse Cedex, France*
† *IBM Research, Zurich Research Laboratory, 8803 Rüschlikon, Switzerland*
‡ *IBM Research, T. J. Watson Research Center, Route 134, Yorktown Heights, New York 10598, USA*

....

The semiconductor industry has seen a remarkable miniaturization trend, driven by many scientific and technological innovations. But if this trend is to continue, and provide ever faster and cheaper computers, the size of microelectronic circuit components will soon need to reach the scale of atoms or molecules—a goal that will require conceptually new device structures. The idea that a few molecules, or even a single molecule, could be embedded between electrodes and perform the basic functions of digital electronics—rectification, amplification and storage—was first put forward in the mid-1970s. The concept is now realized for individual components, but the economic fabrication of complete circuits at the molecular level remains challenging because of the difficulty of connecting molecules to one another. A possible solution to this problem is 'mono-molecular' electronics, in which a single molecule will integrate the elementary functions and interconnections required for computation.

A viram and Ratner[1] suggested that a single molecule with a donor–spacer–acceptor (d–s–a) structure (see **1** in Fig. 1c) would behave as a diode when placed between two electrodes: electrons can easily flow from the cathode to the acceptor, and electrons from the donor are then transferred to the anode. The working principle of this device is analogous to that underlying the "valve" effect introduced by Schockley 60 years ago[2], but involves manipulating the electronic wavefunction of the metallic electrodes extending through the d–s–a molecule, rather than the carrier density in a semiconductor material. Such hybrid molecular electronic (HME) devices, comprising molecules embedded between several electrodes, thus differ radically from bulk-material-based molecular electronic technologies found in applications such as dye lasers, light-emitting diodes, liquid-crystal displays, and soft plastic transistors. However, the design of functional devices and machines based on the molecular electronics concept poses the challenge of integrating the functions required for advanced processing, particularly computing, within the same molecule in a mono-molecular electronics (MME) approach.

Owing to the lack of suitable technologies for establishing electrical contact between individual molecules, experimental investigations of the fundamental processes involved in electron transfer through molecules have long focused on gas-phase and liquid-phase systems. Although these approaches cannot result in working nanoscale devices[3], they have established that a simple shift in the energy of a molecular orbital—induced, for example, by a photo-isomerization—can fine-tune the intramolecular electron transfer rate through an individual molecular bond connecting two redox centres. Experimental studies involving averaging over many isolated molecules have, for example, demonstrated long-range through-bond electron transfer processes in molecule **2** (Fig. 1a)[4,5], intramolecular light-induced conformation changes in molecule **3** (Fig. 1b)[6], and intramolecular interference effects in molecule **4** (Fig. 1b)[7].

Electrical addressing of molecules

Langmuir–Blodgett (LB) and self-assembly fabrication techniques[8] can be used on many molecules to form organized molecular monolayers on suitable substrates. This allowed Mann and Kuhn to investigate long-range tunnelling through alkane chains in ordered LB monolayers[9]. Similarly, sandwiching molecule **5** (Fig. 1c) between differing metallic electrodes allowed the first (albeit somewhat ambiguous) observation of rectification effects in a molecular monolayer[10], confirmed by subsequent work[11] using molecule **6** (Fig. 1c) sandwiched between electrodes made from the same material.

The scanning tunnelling microscope (STM) enables controlled two-terminal measurements, and its development has thus allowed new experimental approaches for demonstrating and probing electron transport through individual molecules[12]. Examples include the electrical single-atom switch realized using a Xe atom[13] at cryogenic temperatures and the first experimental determination of the electrical contact point of a single C_{60} molecule (ref. 14). The resistance of $R = 55\,M\Omega$ obtained in the C_{60} experiment corresponds to an electronic transparency (ease of transmission) of $T = 2.3 \times 10^{-4}$, with T being approximately proportional to the square of the inter-electrode electronic coupling introduced by the molecule compared to the corresponding vacuum gap. Ohmic dissipation in the electrodes is one way to evaluate T from the macroscopically measurable quantity R, as $T = h/2e^2\, R^{-1}$. However, owing to R being the resistance of the metal–C_{60}–metal tunnel junction, rather than that of the C_{60} molecule, it cannot be used to define molecular conductivity.

STM measurements on C_{60} have revealed linear current–voltage (I–V) characteristics at low applied bias voltages[14], indicating that the system behaves similarly to a metal–vacuum–metal tunnel junction at low bias voltage. However, 'squeezing' a C_{60} molecule by applying a small force in the nanonewton range with a metallic STM tip results in a shift of the molecular orbital levels[14]. This mechanically induced shift provides a means to modulate tunnelling through a single C_{60} molecule, even in a nonresonant tunnelling regime, and to change its resistance up to a limiting value approaching the quantum of resistance, $h/2e^2$ ($\sim12.9\,k\Omega$) (ref. 14). The phenomenon, mechanically modulated virtual-resonant tunnelling (VRT), has also been used to design an electromechanical amplifier (Fig. 2a), by making use of the ability to mechanically reduce molecular level degeneracy[15]. Specific to highly degenerate systems, the electomechanical amplifier is the tunnelling equivalent, on the nanometre scale, of the Schockley "valve" effect[2].

A variety of other techniques, such as experiments based on Coulomb blockade[16], nanopore[17], break junction[18,19], electrodeposition[20] and nanolithography[21,22], have been used to determine

541

the electronic transparency of single molecules whose configuration approaches the planar wiring configuration encountered in semiconductor devices. Coulomb blockade work on molecule **7** (Fig. 1a), for example, used a tunnel-capacitor model for the metal–molecule–cluster STM junction used to estimate a tunnelling resistance R from the experimental data and extract the corresponding transparency T, yielding $R = 9\,M\Omega$ and $T = 1.4 \times 10^{-3}$ (ref. 16). The 'nanopore' technique consists of fabricating holes of very small diameter in a suspended silicon nitride membrane equipped with a metallic electrode in its base. The pores are then filled with molecules and a second metallic electrode is evaporated on top of the device[17]. For molecule **8**, Fig. 1a, nonlinear two-terminal $I-V$ characteristics were recorded, and $R = 150\,M\Omega$ was estimated at low voltage[17]. Break junctions involve the gentle fracture of a microfabricated electrode in its centre by mechanical deformation while measuring the resistance of the metallic wire junction[23]. Its application to single molecules is difficult because a liquid evaporation step is required after formation of the junction, and the
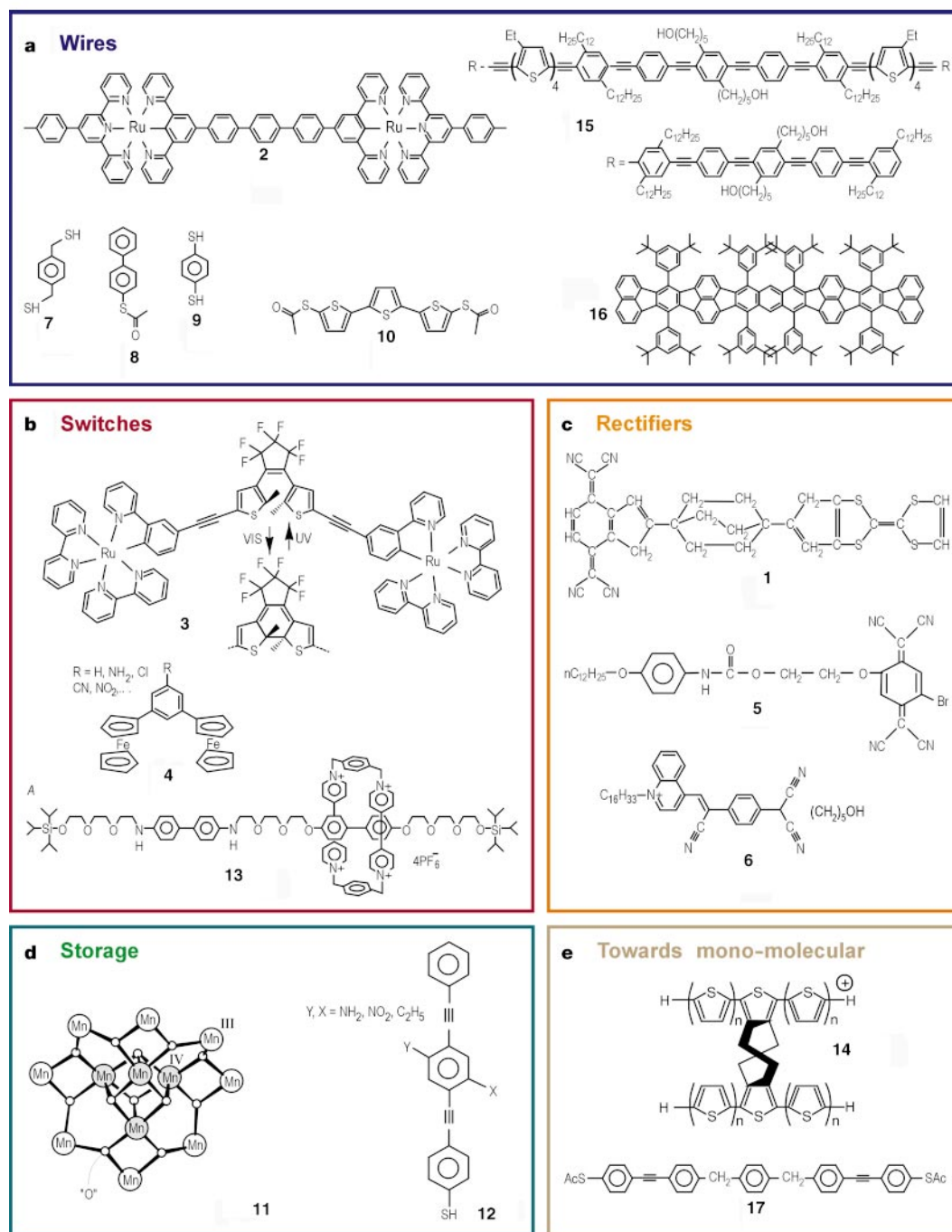
Figure 1 The molecules described in the text. **a**, Wires; **b**, hybrid molecular electronic (HME) switches; **c**, HME rectifiers; **d**, storage; and **e**, two molecules that show promise for mono-molecular electronics. Only the manganese acetate molecule **11** of formula $(Mn_{12}O_{12}(CH_3COO)_{16}(H_2O)_4$ is not completely represented, for clarity[48]. All these molecules have been synthesized apart from the historical design **1** of a d–s–a molecular rectifier[1]. Molecules **14** and **15** have not yet been characterized. **14** is the first proposal of an intramolecular transistor and **17** is an intramolecular quantum well.

conformation and the exact number of interconnected molecules remain essentially inaccessible[19]. Nevertheless, measurements have provided estimates of $R = 22$ MΩ ($T = 5.9 \times 10^{-4}$) for a junction containing molecule **9** shown in Fig. 1a (ref. 18). In the case of molecule **10** (Fig. 1a) and its dimer, values of $R = 12.5$ MΩ ($T = 1.03 \times 10^{-3}$) and $R = 160$ MΩ ($T = 7.7 \times 10^{-5}$) were obtained, respectively[19].

Electro-deposition techniques[20] use suspended electrodes in a pseudo-planar configuration to trap molecules electrostatically in and onto the junction. Interrupting the trapping field at the first observed increase of the current in the circuit leads to the deposition of a finite number of molecules in the junction. This approach is similar to break junctions, but there are no imaging methods available to verify the actual number and orientation of the molecules in the junction. Using this configuration, an oligonucleotide straddling an 8-nm nanojunction was found to be negligibly electrically conducting up to an applied potential of several volts[24].

Nanolithography has made important contributions towards using mesoscopic electrodes[25,26] and nanojunctions for HME[27]. The measurement of the conductance of single-wall carbon nanotubes (SWCNTs) represented the observation of molecular-scale objects electrically interconnected in a full planar configuration, together with images of the position and conformation of the macromolecule[25,26]. SWCNTs with appropriate helicity were found to transport electrons ballistically[25], that is, their electronic transparency is $T = 1$. Consequently, the conductance of the metal–SWCNT–metal junction is determined by the metal–SWCNT contacts. It has generally been difficult to decrease contact resistances in these systems below 100 kΩ (ref. 28), but the use of catalysts to pattern and grow SWCNTs directly onto electrodes has recently resulted in two-terminal contact resistances as low as a few kilo-ohms (ref. 29).

At low voltages, two regimes of elastic transport explain the large scatter of transparency values measured on single molecules. (Transport can involve either electrons or quasi-particles, such as polaron and soliton carriers.) For $T > 1$, the transport regime is ballistic: the molecular levels are in resonance with the Fermi level of the electrodes, and there is complete electronic delocalization along the molecule. In the case of SWCNTs at low temperatures[30], the transport coherence length can extend to as much as 500 nm (Fig. 3). Values of $T < 1$ indicate that either the molecule is differently bound to the electrodes or that the Fermi level is located within the gap between the highest occupied (HOMO) and the lowest unoccupied (LUMO) molecular orbitals. In the first case, the tunnelling regime is determined by the metal–molecule contact, which can be optimized by controlling the surface chemistry. To overcome the second situation, the molecular orbitals need to be electronically coupled to the electrodes to stabilize a tunnel pathway for the carriers that is more efficient than vacuum. This pathway builds up from the constructive or destructive superposition of tunnel channels. For C_{60} adsorbed on the Au(110) surface, this involves 36 of a total of 240 molecular orbitals[14]. For systems with $T < 1$ and involving a molecule symmetrically chemisorbed on the electrodes, such as C_{60} bound to two similar electrodes, two-terminal measurements exhibit linear $I–V$ characteristics when V is much lower than the molecule's effective barrier height[14,19]. This Simmons tunnelling regime is analogous to electron tunnelling between metals at low voltages, also resulting in linear $I–V$ curves. Nonlinear $I–V$ curves usually occur at higher voltages in systems with $T > 1$ involving a physiosorbed molecule[31,32], owing to the contact tunnel barriers at the electrodes dominating the behaviour of the system[25].

Calculations support a very fine dependency of the metal–molecule–metal junction resistance on the chemical structure of the molecule[33,34], its conformation in the junction[35], and its chemical binding to the electrodes[33,36,37]. In these calculations, the electronic and mechanical description of the junction includes the atomic structure of the electrode and the molecular conformation obtained from semi-empirical[38] or, more recently, from density-functional approaches[39]. The tunnelling current intensity is usually derived from the Landauer formula[14], with the scattering problem being solved using a spatial propagator[40] or a Lippman–Schwinger technique through its kernel (Green's function)[41]. Alternatively, the current intensity can be calculated from a time-dependent approach that relates the electron transfer process through the
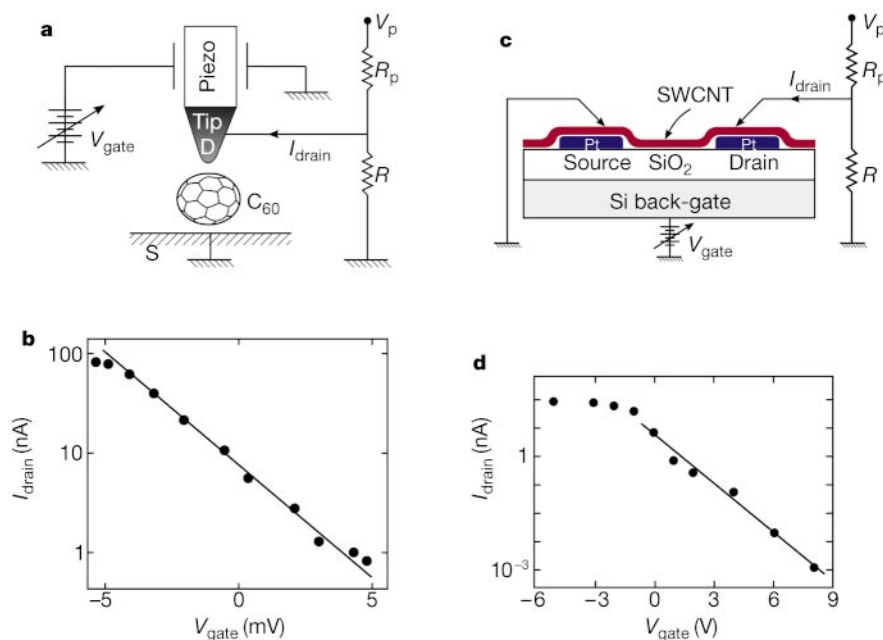

Figure 2 The first two active three-terminal devices in molecular electronics. **a**, **c**, Electrical circuits of **a**, the electromechanical single C_{60} amplifier (in its original scanning tunnelling microscope version[15]) and **c**, the single-wall carbon nanotube (SWCNT) channel transistor[63] with their respective $I_{drain} = f(V_{gate})$ characteristics (S, source; D, drain; I_{drain}, the tunnel current intensity through the molecule). From **b**, the transconductance dI_{drain}/dV_{gate} of the C_{60} amplifier is $g = 3.9 \times 10^{-6}$ A V^{-1} and from **d**, that of the SWCNT transistor is $g = 8 \times 10^{-9}$ A V^{-1}. Those values must be compared to $g = 30 \times 10^{-3}$ A V^{-1} for a bipolar transistor and $g = 3 \times 10^{-3}$ A V^{-1} for a vacuum-tube triode. The channel of these HME devices (**a**, **b**) is truly molecular in scale, but not the grid.

molecule to the rate at which the junction electrodes deliver tunnelling electrons to the molecule[42].

Single hybrid molecular devices

Quasi-ideal rectification characteristics in nanometre-scale objects have been experimentally observed, by sliding an STM tip along a SWCNT[43] and in electrically contacted MWCNTs[44]. More recently, a single, planar SWCNT comprising tube sections with different tube helicities, one conducting and the other semiconducting and with a kink at the intervening junction, was shown to exhibit rectification behaviour on the molecular scale[45]. Molecular oligomers should also behave as d−s−a HME rectifiers, with dimensions well below 10 nm (ref. 1), and experimental proof for the validity of the d−s−a design principle has been obtained[10,11]. But despite these promising advances, many challenges remain: current technologies do not yet permit the realization of planar single-molecule d−s−a rectifiers fabricated with nanometre-scale dimensions, and whether those SWCNT devices can be scaled down by reducing the inter-electrode distance well below 10 nm remains an open question[46]. Similarly, rectification effects observed in nanopores[17] using molecule **8** (Fig. 1a) and in organic heterostructures[47] still involve several thousand molecules, making it difficult to assess to what extent scaling to a single-molecule level will be possible.

Hysteresis behaviour is a useful property for information storage applications. Manganese acetate (molecule **11** in Fig. 1d), with a total spin magnetic moment of 20 μ_B is the first molecule shown to exhibit a hysteresis cycle under cryogenic conditions[48]. Because magnetic hysteresis is usually seen as a collective property of bulk material, magnetic phenomena associated with single atoms[49] or molecules[50] have attracted much interest in the context of device scaling and quantum micro-reversibility[51]. An alternative approach to storage is to build devices that display negative differential resistance (NDR)[52], that is, a negative slope in their I−V curves like the one exhibited by a tunnel diode. Introduced in a two-terminal device, molecules exhibiting NDR play the equivalent role of a nonlinear material in photonic Fabry−Perot resonators showing a hysteresis cycle[53]. NDR with a high peak-to-valley ratio was observed[54] for molecule **12** (Fig. 1d).
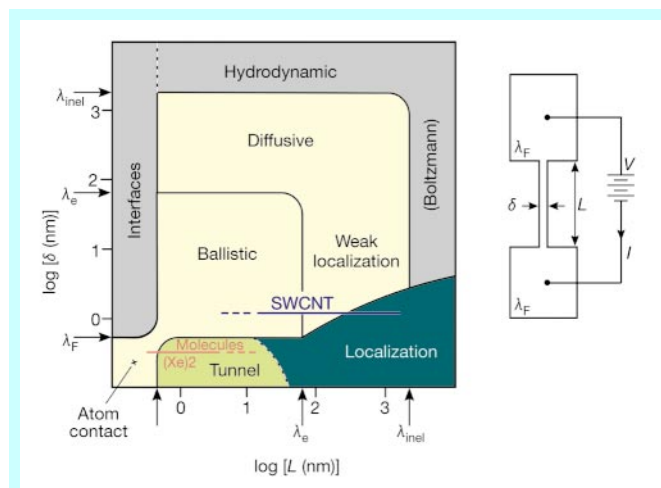
Figure 3 Regimes of electronic transport as a function of the wire width δ and length L. λ_F is the de Broglie carrier wavelength in the contact electrodes (away from the constriction), λ_e the elastic mean free path in the wire and λ_{inel} the inelastic mean free path in the wire. Characteristic orders of magnitude for λ_F, λ_e and λ_{inel} are taken for noble metals at low temperature. Hydrodynamic (Boltzmann), diffusive (weak localization) and ballistic regimes have been well studied in the past for metals and semiconductors. Ballistic and weak localization regimes are now being studied on SWNTs[25], atomic metallic wires[23] and the tunnel regime on single molecules[14,18,19,76] and short atomic wires[96].

Suggestions[55−58] for single-molecule molecular switches have been put forward for some time, but relatively few have been synthesized[6,59]. In an electronic circuit, switching is based on an intrinsic molecular property involving a bistable change of internal structure (such as a conformation change[57] or a unimolecular reaction[6,59]), which induces a modification of T. For example, the photochromic switching of molecule **3** (Fig. 1b) is possible because a photo-induced molecular orbital "up-shift" in the "on" state[6] favours efficient electron transfer through **3**, making this phenomenon an intramolecular analogue of the solid state "valve" effect. Rotaxanes **13** (Fig. 1b) have also been proposed as mechanical molecular switches[60]: the macromolecular ring can move along the molecule's central 'axle' and occupy one of two or more metastable positions or 'stations' along the axle, where one position provides a high-T and the other a low-T state. The gating used for these two switches has a macroscopic origin (light for the photochromic effect, pH and light control for the rotaxane), but the development of near-field integrated optics[61] may provide a more controlled means to optically gate molecular switches on the mesoscopic scale.

Proposals of HME transistors are numerous[62], yet their realization[55] remains challenging because logic circuit applications require a three-electrode configuration with high gain. SWCNTs have been used as the channel of a field-effect transistor[63], but the device is still mesoscopic in dimension because it operates by controlling the Schottky barrier height at the single-wall nanotube (SWNT)−electrode contacts (Fig. 2b). Plans to move the control of transparency T from the contact between the active molecule and the electrodes to the active molecule itself involve the electro-mechanical amplification effect of C_{60} (Fig. 2a), which might be planarized[64] using nano-electromechanics (NEMS)[65]. Oxidation−reduction processes provide another way of controlling the transparency of a molecular tunnel pathway. For instance, conjugated molecules such as polyacetylene, polythiophene or polypyrrole conduct with T > 1 when a few electrons are removed or added to introduce electronic states in the HOMO−LUMO gap of the molecule generally in resonance with the electrode Fermi level, at low bias voltage. Using a perpendicular electric field, those electrons can be driven from one molecular chain to another (molecule **14** in Fig. 1e), acting as a transistor source−drain channel[66]. Synthetic work has produced a number of spiro-bridge compounds (such as **14**)[67] that confirm the presence of an electronic double-well potential at the bridge site[68]. As in many designs employing electromechanical, electrical-field or even electronic interference effects[69], the third electrode, which gates the HME transistor, is mesoscopic and not readily scalable to nanoscale dimensions. Coulomb-blockade devices[16] and molecular junctions consisting of two different molecular components[35,47] have similar scalability problems.

Architecture of hybrid molecular electronic circuits

Given the proposed mode of operation of HME devices and reliability issues, circuit design is emerging as a crucial aspect in the development of future molecular electronic systems, with input/output interconnects, clock frequency and the increase of logic complexity constituting particularly challenging problems. Although NEMS technology may represent a potential solution to reduce the area occupied by the interconnection pads on a wafer, the bandwidth of these interconnects is limited to a few megahertz. The potential switching rate of the molecular component in an HME device, in contrast, is of the order of several terahertz[15,63], but it may require optical interconnects, such as subwavelength photonic waveguides[61], to use these frequencies.

Continuation of the 'top-down' approach indicates that a conservative architecture with metallic wires interconnecting many devices to form a complex network is feasible using well-defined and spatially localized logic gates, registers and memory cells (Fig. 4). In this case, high-gain three-terminal HME devices are essential for

fan-out (the ability of a given device to provide sufficient power to operate multiple devices interconnected to it) to reduce the wiring complexity between the gates and to lower the power dissipation per gate. The extreme fabrication constraints, especially for complex circuits, will require new architecture paradigms. For instance, it has been proposed to replace process precision by software precision[70], by using an external nonmolecular processor to select the working HME devices from a massive array of HME devices connected in a chequerboard pattern and to configure a particular circuit. In such cases gain might be localized elsewhere, using traditional CMOS (complementary metal oxide semiconductors) outside the molecular electronic circuitry, with some trade-off in space. Other architectures that have been proposed are quantum cellular automata[55,71] and quantum computing using a molecule as a quantum dot[72].

Mono-molecular integration

An ultimate limit of downscaling a circuit made of metallic wires interconnecting HME devices is a circuit where the wires and devices are no longer distinguishable as localized discrete elements of the circuit. This occurs when the interdevice wire length is well below the electronic phase coherence length of the wire material, so that the circuit operates in a ballistic regime where a minute difference between device positioning or wire length will render the circuit unreliable[73]. Another limit, also experienced in integrated photonics[74] and mesoscopic low-temperature devices[75], is that true intrinsic three-terminal devices with external grids are difficult to design in a ballistic regime. A similar problem arises when a metallic control electrode is used to gate a single HME device (Fig. 2). Therefore, the scaling ability of the HME approach is limited even if SWCNTs are used to replace the metallic nanowires for interdevice wiring. Semiconductor-based electronics, when faced at the end of the 1950s with similar limitations that were based on different physical constraints, turned to monolithic technology, which integrates the wiring, transistors and the required passive elements on a single piece of silicon. The conceptually comparable mono-molecular approach (MME) was suggested for molecular electronics as early as the 1980s[55], but has only recently received serious

theoretical[40] and experimental consideration[45,76]. Tunnelling is one way to overcome the limitations associated with the ballistic transport regime. In this case, electrons are channelled from one reservoir to the other via a network of tunnelling pathways defined by atomic or molecular wires.

The tunnel transparency T between two metallic electrodes is known to exhibit a sharp exponential decay, $T = T_0 e^{-\gamma L}$ with length L through a vacuum gap and $\gamma \simeq 2\,\text{Å}^{-1}$ (ref. 77). Low-gap semiconductor[78] or molecular materials[9] tend to reduce the inverse decay length γ. It has been shown theoretically[79] that tunnelling currents as high as 10 pA under a 0.1-V bias voltage can be driven through specifically designed molecular wires having lengths exceeding 10 nm and a HOMO–LUMO gap in the 1-eV range. Recently, a value of $\gamma = 0.4\,\text{Å}^{-1}$ was reported for the molecular wire **16** (Fig. 1a), equipped with supporting molecular groups (legs) that exhibit very low T that protect the conjugated wire from a Cu(100) surface. One end of the molecular wire was interconnected to a double atomic step edge and a STM tip used to explore the length dependence of its transparency[76], confirming that tunnelling electrons can be guided by long molecular wires with an effective section well below 1 nm^2. On the electronic transport regime map (Fig. 3), this 'super tunnel'-like phenomenon corresponds to a wire with a section smaller than the de Broglie wavelength of the electron. It can be interpreted as a permanently driven super-exchange electron-transfer mechanism. Although large-scale theoretical and chemical synthesis efforts are required to model and explore this regime, theoretical considerations indicate that values of γ down to 0.05 Å^{-1} are achievable for a HOMO–LUMO gap in the 1-eV range[79]. Currently, the chemical synthesis strategies for molecular wires continue to place an emphasis on the length (Fig. 4), such as in **15** (Fig. 1a), rather than on the optimization of their γ values.
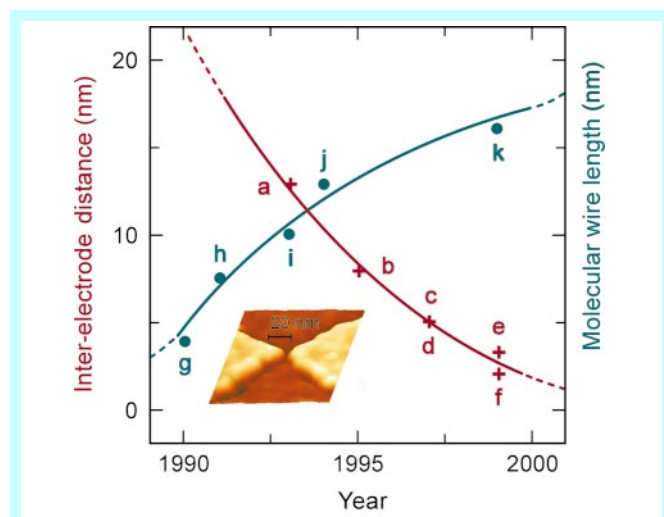
Many calculations have explored the possibility of optimizing the electronic contacts between the end of a molecular wire and a metallic electrode, as has been realized in the case of molecule **16** (ref. 76), by investigating the influence of the wire's end group[33,36,37]. The metal–molecule contact results from a mixing of the end part of the wire's molecular orbitals (HOMO, LUMO and the others
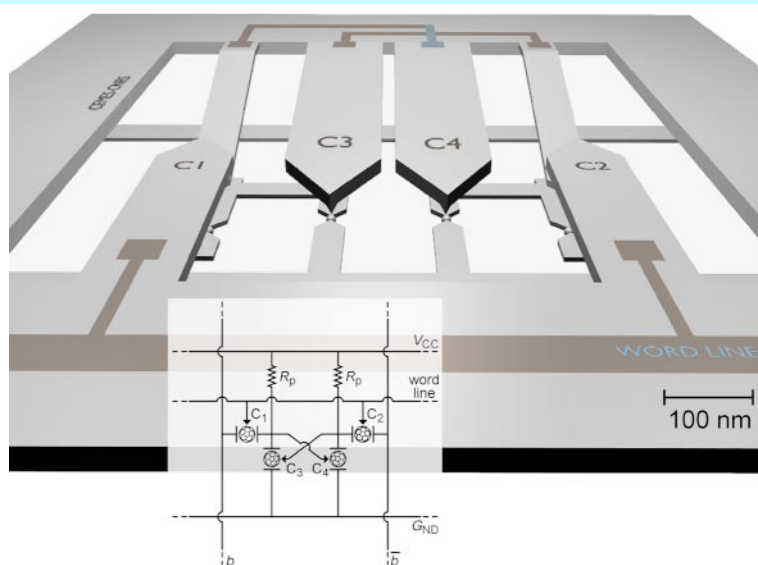
Figure 4 Representative example design of a hybrid molecular electronic device. The figure shows the layout of a memory cell that consists of four individual C$_{60}$ electromechanical transistors[64] (two for the trigger and two for the driving transistors) under a bias voltage V_{CC} with respect to ground, G$_{ND}$. The top part is made of four nanoelectromechanics (NEMS) grids plus two metallic NEMS cantilevers, and the lower part is the electrical polarization circuit with polarization resistances R_p made using a metallic constriction along the mesoscopic metallic wires of the circuit (see inset). The full circuit was simulated and optimized using an equivalent electrical circuit for each cantilever and for each C$_{60}$ molecule using the known C$_{60}$ experimental electrical characteristics upon compression[15]. Inset, the equivalent electrical circuit diagram. b and $\bar{b}$ carry the digital information to be stored in a memory cell, and the word line activates a line of memory cells for a storage operation.

supporting the tunnel path) with the surface metallic orbitals of the contacts. The resulting extension of the metallic wavefunction of the electrode into the molecular wire may be viewed as a doping effect[37] without introducing states in the HOMO–LUMO gap. In the STM images of molecules adsorbed at steps, the apparent height of the molecule is a clear measure of the quality of the electronic contact with their metallic step, which acts as an electrode. This accounts for the pre-factor T_0 in the expression for the tunnel transparency and provides a quantitative criterion for optimizing the metal–molecule contact.

Intramolecular circuits can be formed without metallic pads by using molecular wires. Contrary to conventional electrical circuits, where adding one branch does not change the electronic properties of the others, any new molecular wire or branch added to a molecule effectively creates a 'new' molecule with a different electronic structure. Therefore, a standard circuit analysis resulting from the application of Ohm's and Kirchhoff's laws is inapplicable even if the design of molecular logic continues to be based on those laws[80]. From elastic scattering theory, the chemical binding of two oligomers with low transparencies T_1 and T_2 in series gives a total transparency T proportional to $T_1 \times T_2$. The binding of two or more oligomers in parallel requires two auxiliary branches to form the nodes (Fig. 6). In this case and when $T < 1$ for each branch, the superposition law yields $T = T_h + T_b + 2(T_h \times T_b)^{1/2}$ (ref. 40) with T_h and T_b being the transparency of each complete individual branch (Fig. 5). However, it is not yet clear whether the invalidity of standard circuit analysis derives solely from the inapplicability of Ohm's law, emphasizing the need for experimental investigations of intramolecular currents. Nanopore measurements on molecule **17** (Fig. 1e), which consists of three conjugated branches associated in series via two non-conjugated CH_2 nodes[80], have revealed a very small NDR effect attributed to the central phenyl ring, indicating a multiplicative rather than additive superposition for an association in series. In order to probe along each branch of an intramolecular circuit, large and multi-branched macromolecules[81] need to be synthesized (and imaged), indicating that the fabrication precision

in MME can then be combined by chemical synthesis and nano-fabrication techniques, a process referred to as directed self-assembly.

Intramolecular devices will need to be controlled internally without crosstalk to adjacent molecules. Suitable intramolecular wiring and circuitry[55,80,82] has been proposed, but an intrinsic gating effect that allows internal control has not yet been identified. Even SWCNTs crossing each other[83] or junctions[45] on the molecular scale are typically gated with an electrode connected to a macroscopic pad, suggesting that intramolecular electronic wavefunctions might need to be manipulated differently, such as is done in quantum computing to perform computation inside a single molecule. However, the laws governing the physics of an intramolecular circuit in the tunnelling regime are poorly known. Although it might be possible, for example, to use the vibronic pseudo-continuum associated with many electronic states of a large molecule to break microreversibility and thus design intrinsic three-terminal devices, we cannot yet test this idea directly owing to the difficulties in observing inelastic effects experimentally[84]. Electron correlation effects have now been observed in MWCNTs[30] and SWCNTs[85], but further advances in this direction are required to determine whether a full mono-molecular approach is technologically viable and thus able to provide a realistic alternative to monolithic silicon devices.

Nanofabrication

The fabrication of a circuit using HME devices or the interconnects of MME devices requires the following steps: (1) fabrication of millions of multi-electrode nanojunctions with interelectrode distances down to a few nanometres; (2) wiring these junctions to interconnects; (3) deposition/assembly of one molecule or super-molecule per nanojunction; (4) fabrication of the input/output and driving power interconnects; and (5) packaging the circuit. Currently, two-electrode nanojunctions down to 5 nm have been produced by electron-beam nanolithography, and electrodeposition techniques have revealed that 2 nm can be reached (Fig. 5). Two nearby SWCNTs have also been used to define a nanojunction using
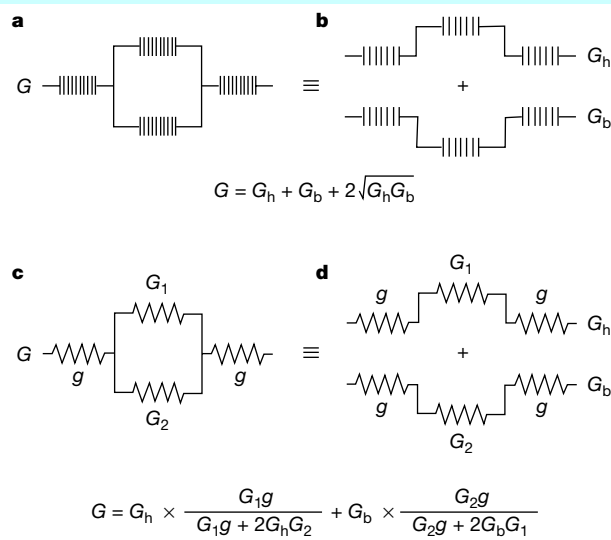

Figure 5 Variation of the inter-electrode distance of planar nanojunctions and the length of the synthesized molecular wires as a function of time. Red, inter-electrode distance; green, molecular wire length. **a, b**, Planar standard e-beam nanolithography nanojunctions, ref. 97 (**a**) and ref. 22 (**c**). **b, e**, Co-planar e-beam nanojunctions with the electrode metal at the same height as the substrate, ref. 21 (**b**) and ref. 27 (**e**). **d, f**, Suspended planar nanojunctions fabricated by electrodeposition[98] (**d**) and electrochemistry[99] (**f**). **g, h**, Long oligoimide molecular lines, ref. 100 (**g**) and ref. 101 (**h**). **i**, Thiophene-ethynylene oligomers[102]. **j**, Phenylalkyne oligomers[103]. **k**, Alternating block co-oligomers of (1,4-phenylene ethynylene)s and (2,3-thiophene ethynylene)s[104]. Inset, AFM tapping mode image of a 4-nm coplanar nanojunction. In **e**, the two gold-palladium metal electrodes are only 1 nm higher than the background silicon wafer surface[27].

Figure 6 Illustration of the superposition rule operating in a pure tunnelling regime for a simple intramolecular circuit. **a**, The circuit is made of a molecule composed of two branches bonded in parallel and connected to the pad through molecular wires. **b**, The full conductance G of the metal–molecule–metal junction is obtained by decomposing the circuit into two parts having junction conductances G_h and G_b, respectively, and summing up G_h and G_b as indicated (the same rule applies for the transparencies). **c**, By comparison, the conductance G of the same circuit, but with conventional ohmic resistances g, G_1 and G_2, can also be decomposed in this way (**d**). Of course, this decomposition is never used in circuits, and G for **c** is better calculated using standard circuit analysis.

templates[29]. For interconnect wiring, a number of approaches exist that go beyond current ultraviolet (UV) or electron-beam lithography. For example, wiring can be nano-imprinted with a resolution limit of more than 10 nm[86], realized with SWCNTs, or "nanostencilled"[87] in high vacuum by using movable shadow masks and apertures in cantilevers or a thin silicon membrane when depositing the metallic wires from a source of metal atoms and/or molecules. In addition to being a resist-free, ultraclean nanolithography technique, nanostencilling is a parallel process that allows the simultaneous use of several thousand apertures. Arrays of electron-beam microcolumns are also being developed for parallel nanolithography technology with a resolution of about 10 nm (ref. 88). The array provide low-voltage electron-beams and increase the throughput, with one microcolumn being responsible for each HME circuit or MME circuit interconnection. The accurate placement of molecules in the appropriate position and orientation to form a device, or building of a small circuit with a few SWNTs[89], is readily achieved through molecular manipulation using scanning-probe microscopy (SPM). But turning this approach into a parallel process will most probably involve patterning of the molecules on surfaces using 'wet' methods, such as self-assembly, combing, cantilever techniques, nanostamping or nanostencilling. Self-assembly is a particularly attractive strategy because it could, in principle, exploit thermodynamic control to achieve high precision[90], but the overall precision with which complex structures can be assembled through molecular self-organization remains to be investigated. Currently, molecular combing can reach a 40% rate of success in connecting SWCNTs[91] between two electrodes. It relies on the force exerted by a liquid meniscus on the SWCNT adsorbed on the wafer and requires a chemical preparation of the wafer surface, a process accessible to nano-imprinting, but not yet applied to oligomers. Nanostamping uses elastomeric stamps made with a pattern of reliefs on their surface. After 'inking'—a term used to describe the coating of the stamp with molecules—the stamp is contacted to a surface, which allows the accurate reproduction of their area of contact by leaving behind a patterned molecular monolayer in a manner similar to printing[105,106]. It can attain a precision of a few nanometres but requires that surface and gas phase diffusion be controlled. Shadow masks are well adapted for ultraclean processes[87], but suitable molecular sources need to be further developed to take into account the MME circuit requirement towards higher molecular weights. Experiments have already explored the use of nonthermal sublimation methods such as matrix-assisted laser desorption (MALD)[92] or injection of aqueous solutions of molecules into ultrahigh vacuum[81]. The ultimate limits of fabrication will probably require the development of "directed self-assembly" methods, where a finite number of molecules or atoms can be assembled and deposited at predefined locations[93]. Self-assembly, directed by molecular recognition, provides a very efficient means to construct helices, and rack, ladder and grid structures[94], and provided suitable assembly and electronic functions are "pre-installed" into a molecule during synthesis, it may be used for the self-positioning of HME devices or MME circuits.

Quantum machines

The first proposals for molecular electronics appeared in the 1970s, but it is only the appearance of a number of scientific and economic developments that has allowed the recent resurgence of activity in this field. Crucial are advances in nanoscale science and technology, such as new fabrication methods and probes, which enable individual molecules or small numbers of molecules to be connected in a controlled manner into actual test devices. The driving force behind this research is clearly the need for suitable alternative technologies to Si-based CMOS, which is expected to reach its limitations in 10–20 years[71]. Our understanding and concepts of what molecular electronics might look like in the future have changed significantly as a result of all of these factors. In particular, electrode effects and the extreme sensitivity of quantum tunnelling to small atomic motions, and switching behaviour and rotation[95] in single molecules, are good examples of possible new operational methodologies that have appeared in the past five years. Finally, the understanding and control of directed self-assembly techniques, combined with developments in synthetic and supramolecular chemistry, increasingly focus on the notion that molecular devices and machines can be synthesized from first principles. The logical progression of this approach is mono-molecular electronics, which integrates many electronic elements, such as wires, switches, and amplifiers, in a single molecule or individual supramolecular assembly. There are many unresolved issues and opportunities for molecular electronic devices in the areas of architecture where a conventional analysis of a molecular device in terms of the linear superposition of its components appears to be invalid. This may make molecular electronics a prime contributor to the building of nanoscale quantum machines using the power of quantum-state superposition. Indeed, as synergistic and cooperative effects in complex molecular systems are understood and controlled, new electronic devices based on unconventional operating principles might be developed. In short, it seems that applying conventional electronic concepts and approaches will not necessarily be the best way to achieve functional molecular devices operating on a dimensional scale where quantum mechanics dominates. □

1. Aviram, A. & Ratner, M. Molecular rectifiers. *Chem. Phys. Lett.* **29**, 277–283 (1974).
2. Riordan, M. & Hoddeson, L. *Crystal Fire: The Birth of the Computer Age* (W. W. Norton & Company, New York, 1997).
3. Taube, H. The electron transfer between metal complexes: a retrospective. *Science* **226**, 1028–1036 (1984).
4. Patoux, C. *et al.* Long-range electronic coupling in bis(cyclometalated) ruthenium complexes. *J. Am. Chem. Soc.* **120**, 3717–3725 (1998).
5. Davis, W. B., Svec, W. A., Ratner, M. A. & Wasielewski, M. R. Molecular-wire behaviour in p-phenylenevinylene oligomers. *Nature* **396**, 60–63 (1998).
6. Fraysse, S., Coudret, C. & Launay, J.-P. Synthesis and properties of dinuclear complexes with a photochromic bridge: switching "ON" and "OFF" an intervalence electron transfer. *Eur. J. Inorg. Chem.* 1581–1590 (2000).
7. Patoux, C., Coudret, C., Launay, J.-P., Joachim, C. & Gourdon, A. Topological effects on intramolecular electron transfer via quantum interference. *Inorg. Chem.* **36**, 5037–5049 (1997).
8. Delamarche, E., Michel, B., Biebuyck, H. A. & Gerber, C. Golden interfaces: the surface of self-assembled monolayers. *Adv. Mater.* **8**, 719–729 (1996).
9. Mann, B. & Kuhn, H. Tunnelling through fatty acid salt monolayers. *J. Appl. Phys.* **42**, 4398–4405 (1971).
10. Geddes, N. J., Sambles, J. R., Davis, D. J., Parker, W. G. & Sandman, D. J. Fabrication and investigation of asymmetric current-voltage characteristics of a metal/Langmuir-Blodgett mono-layer/metal structure. *Appl. Phys. Lett.* **56**, 1916–1918 (1990).
11. Metzger, R. M. *et al.* Unimolecular electrical rectification in hexadecylquinolinium tricyanoquino-dimethanide. *J. Am. Chem. Soc.* **119**, 10455–10466 (1997).
12. Gimzewski, J. K., Stoll, E. P. & Schlittler, R. R. Scanning tunnelling microscopy on individual molecules of copper phthalocyanine adsorbed on polycrystalline silver surfaces. *Surf. Sci.* **181**, 267–277 (1987).
13. Eigler, D. M., Lutz, C. P. & Rudge, W. E. An atomic switch realised with the scanning tunnelling microscope. *Nature* **352**, 600–603 (1991).
14. Joachim, C., Gimzewski, J. K., Schlittler, R. R. & Chavy, C. Electronic transparence of a single C_{60} molecule. *Phys. Rev. Lett.* **74**, 2102–2105 (1995).
15. Joachim, C. & Gimzewski, J. K. An electromechanical amplifier using a single molecule. *Chem. Phys. Lett.* **265**, 353–357 (1997).
16. Dorogi, M., Gomez, J., Osifchin, R., Andres, R. P. & Reifenberger, R. Room-temperature Coulomb blockade from a self-assembled molecular nanostructure. *Phys. Rev. B* **52**, 9071–9077 (1995).
17. Reed, M. A. *et al.* The electrical measurement of molecular junctions. *Ann. NY Acad. Sci.* **852**, 133–144 (1998).
18. Reed, M. A., Zhou, C., Muller, C. J., Burgin, T. P. & Tour, J. M. Conductance of a molecular junction. *Science* **278**, 252–254 (1997).
19. Kerguelis, C. *et al.* Electron transport through a metal-molecule-metal junction. *Phys. Rev. B* **59**, 12505–12513 (1999).
20. Bezryadin, A., Dekker, C. & Schmid, G. Electrostatic trapping of single conducting nanoparticles between nanoelectrodes. *Appl. Phys. Lett.* **71**, 1273–1275 (1997).
21. Rousset, V., Joachim, C., Rousset, B. & Fabre, N. Fabrication of co-planar metal-insulator-metal nanojunction with a gap lower than 10 nm. *J. Phys. III* **5**, 1983–1989 (1995).
22. Di Fabrizio, E. *et al.* Fabrication of 5 nm resolution electrodes for molecular devices by means of electron beam lithography. *Jpn. J. Appl. Phys.* **36**, L70–L72 (1997).
23. Yanson, A. I., Yanson, I. K. & van Ruitenbeek, J. M. Observation of shell structure in sodium nanowires. *Nature* **400**, 144–146 (1999).
24. Porath, D., Bezryadin, A., de Vries, S. & Dekker, C. Direct measurement of electrical transport through DNA molecules. *Nature* **403**, 635–638 (2000).
25. Tans, S. J. *et al.* Individual single wall carbon nanotubes as quantum wires. *Nature* **386**, 474–477 (1997).
26. Ebbesen, T. W. *et al.* Electrical conductivity of individual carbon nanotubes. *Nature* **382**, 54–56 (1996).

27. Cholet, S., Joachim, C., Martinez, J. P. & Rousset, B. Fabrication of co-planar metal-insulator-metal nanojunction down to 5 nm. *Eur. Phys. J. Appl. Phys.* **8,** 139–145 (1999).

28. Bachtold, A. *et al.* Contacting carbon nanotubes selectively with low Ohmic contact for four-probe electric measurement. *Appl. Phys. Lett.* **73,** 274–276 (1998).

29. Kong, J., Soh, H. T., Cassell, A. M., Quate, C. F. & Dai, H. Synthesis of individual single-walled carbon nanotubes on patterned silicon wafers. *Nature* **395,** 878–881 (1998).

30. Avouris, Ph. *et al.* in *Proceedings of "Nanotube 1999"* (Plenum, New York, in the press).

31. Mujica, V., Kemp, M., Roitberg, A. & Ratner, M. A. Current-voltage characteristics of molecular wires: eigenvalue staircase, Coulomb blockade and rectification. *J. Chem. Phys.* **104,** 7296–7305 (1996).

32. Porath, D. & Milo, O. Single electron tunnelling and level spectroscopy of isolated C_{60} molecules. *J. Appl. Phys.* **81,** 2241–2244 (1997).

33. Magoga, M. & Joachim, C. Conductance and transparence of long molecular wires. *Phys. Rev. B* **56,** 4722–4729 (1997).

34. Samanta, M. P., Tian, W., Datta, S., Henderson, J. I. & Kubiak, C. P. Electronic conduction through organic molecules. *Phys. Rev. B* **53,** R7626–R7629 (1996).

35. Olson, M. *et al.* A conformation study of the influence of vibration conduction in molecular wires. *Phys. Chem. B* **102,** 941–947 (1998).

36. Yaliraki, S. N., Kemp, M. & Ratner, M. A. Conductance of molecular wires: influence of molecule-electrode binding. *J. Am. Chem. Soc.* **121,** 3428–3434 (1999).

37. Di Ventra, M., Pantelides, S. T. & Lang, N. D. First-principles calculation of transport properties of a molecular devices. *Phys. Rev. Lett.* **84,** 979–982 (2000).

38. Joachim, C. & Vinuesa, J. Length dependence of the transparence (conductance) of a molecular wire. *Europhys. Lett.* **33,** 635–640 (1996).

39. Lang, N. D. & Avouris, Ph. Oscillatory conductance of carbon-atom wires. *Phys. Rev. Lett.* **81,** 3515–3518 (1998).

40. Magoga, M. & Joachim, C. Conductance of molecular wires connected or bonded in parallel. *Phys. Rev. B* **59,** 16011–16020 (1999).

41. Lang, N. D. Resistance of atomic wires. *Phys. Rev. B* **52,** 5335–5342 (1995).

42. Ness, H. & Fisher, A. J. Non-perturbative evaluation of STM tunneling probabilities from ab-initio calculations. *Phys. Rev.B* **56,** 12462–12481 (1997).

43. Collins, P. G., Zetti, A., Bando, H., Thess, A. & Smalley, R. E. Nanotube nanodevices. *Science* **278,** 100–103 (1997).

44. Hu, J. T., Min, O. Y., Yang, P. D. & Lieber, C. M. Controlled growth and electrical properties of heterojunctions of carbon nanotubes and silicon nanowires. *Nature* **399,** 48–51 (1999).

45. Yao, Z., Postman, H. W. Ch., Balents, L. & Dekker, C. Carbon nanotube intramolecular junctions. *Nature* **402,** 273–276 (1999).

46. Léonard, F. & Tersoff, J. Novel length scales in nanotube devices. *Phys. Rev. Lett.* **83,** 5174–5177 (1999).

47. Fischer, C. M., Burghard, M., Roth, S. & von Klitzing, K. Organic quantum wells: molecular rectification and single electron tunnelling. *Europhys. Lett.* **28,** 129–134 (1994).

48. Sessoli, R., Gatteschi, D., Caneschi, A. & Novak, M. A. Magnetic bistability in a metal-ion cluster. *Nature* **365,** 141–143 (1993).

49. Manoharan, H. G., Lutz, C. P. & Eigler, D. M. Quantum mirages formed by coherent projection of electronic structure. *Nature* **403,** 512–515 (2000).

50. Sangregorio, S., Ohm, T., Paulsen, C., Sessoli, R. & Gatteschi, D. Quantum tunnelling of the magnetization in an iron cluster nanomagnet. *Phys. Rev. Lett.* **78,** 4645–4648 (1997).

51. Kahn, O. & Launay, J. P. Molecular bistability: An overview. *Chemtronics* **3,** 140–151 (1988).

52. Mathews, R. H. *et al.* A new RTD-FET logic family. *Proc. IEEE* **87,** 596–605 (1999).

53. Gao, H. J. *et al.* Reversible, nanometer-scale conductance transitions in an organic complex. *Phys. Rev. Lett.* **84,** 1780–1783 (2000).

54. Chen, J., Reed, M. A., Rawlett, A. M. & Tour, J. M. Large on-off ratios and negative differential resistance in a molecular electronic device. *Science* **286,** 1550–1552 (1999).

55. Carter, F. L. The molecular device computer: point of departure for large scale cellular automata. *Physica D* **10,** 175–194 (1984).

56. Higelin, D. & Sixl, H. Spectroscopystudies of the photochromism of N-salicylideneaniline mixed crystals and glasses. *Chem. Phys.* **77,** 391–396 (1983).

57. Joachim, C. & Launay, J. P. Bloch effective Hamiltonian for the possibility of molecular switching in the ruthenium-bipyridylbutadiene-ruthenuim system. *Chem. Phys.* **109,** 93–99 (1986).

58. Hush, N. S., Wong, A. T., Bacskay, G. B. & Riemers, J. R. Electron and energy transfer through bridged systems: VI. molecular switches. *J. Am. Chem. Soc.* **112,** 4192–4197 (1990).

59. Gilat, S. L., Kawai, H. S. & Lehn, J. M. Light-triggered electrical and optical switching devices. *J. Chem. Soc. Chem. Commun.* 1439–1442 (1993).

60. Bissel, R. A., Cordova, E., Kaifer, A. E. & Stoddart, J. F. A chemically and electrochemically switchable molecular shuttle. *Nature* **369,** 133–137 (1994).

61. Girard, C., Dereux, A. & Joachim, C. Photonic transfer through subwavelength optical waveguide. *Europhys. Lett.* **44,** 686–692 (1998).

62. Goldhaber-Gordon, D., Montemerlo, M. S., Love, J. C., Opiteck, G. J. & Ellenbogen, J. C. Overview of nanoelectronic devices. *Proc. IEEE* **85,** 521–539 (1997).

63. Tans, S. J., Verschueren, A. R. M. & Dekker, C. Room temperature transistor based on a single carbon nanotube. *Nature* **393,** 49–52 (1998).

64. Joachim, C., Gimzewski, J. K. & Tang, H. Physical principles of the single C_{60} transistor effect. *Phys. Rev. B* **58,** 16407–16417 (1998).

65. Brugger, J., Beljakovic, G., Despont, M., de Rooij, N. F. & Vettiger, P. Silicon micro/nanomechanical device fabrication based on focused ion beam surface modification and KOH etching. *J. Microelec. Eng.* **35,** 401–404 (1997).

66. Aviram, A. Molecules for memory, logic and amplification. *J. Am. Chem. Soc.* **110,** 5687–5692 (1988).

67. Tour, J. M., Rulian, W. & Schumm, J. S. Extended orthogonally fused conducting oligomers for molecular electronic devices. *J. Am. Chem. Soc.* **113,** 7064–7066 (1991).

68. Diers, J. R. *et al.* ESR characterisation of oligomeric thiophene materials. *Chem. Mater.* **6,** 327–332 (1994).

69. Treboux, G., Lapstun, P. & Silverbrook, K. Conductance in nanotube Y-junctions. *Chem. Phys. Lett.* **306,** 402–406 (1999).

70. Collier, C. P. *et al.* Electronically configurable molecular-based logic gates. *Science* **285,** 391–394 (1999).

71. Compano, R., Molenkamp, L. & Paul, D. J. (eds) *Technology Roadmap for European Nanoelectronics* (European Commission, IST Program, Brussels, 1999).

72. Nakamura, Y., Pashkin, Yu. A. & Tsai, T. S. Coherent control of macroscopic quantum states in a single-Cooper-pair box. *Nature* **398,** 786–788 (1999).

73. Landauer, R. Can we switch by control of quantum mechanical transmission? *Phys. Today* 119–121 (1989).

74. Keyes, R. W. Lighting up logic. *Nature* **362,** 289–290 (1993).

75. Washburn, S., Schmid, H., Kern, D. & Webb, R. A. Normal-metal Aharonov-Bohm effect in the presence of a transverse electric field. *Phys. Rev. Lett.* **59,** 1791–1794 (1987).

76. Langlais, V. *et al.* Spatially resolved tunnelling along a molecular wire. *Phys. Rev. Lett.* **83,** 2809–2812 (1999).

77. Simmons, J. G. Generalized formula for electric tunnel effect between similar electrodes separated by a thin insulating film. *J. Appl. Phys.* **34,** 1793–1803 (1963).

78. Lewickit, G. & Mead, C. A. Experimental determination of the E-k relationship in electron tunnelling. *Phys. Rev. Lett.* **16,** 939–941 (1966).

79. Magoga, M. & Joachim, C. Minimal attenuation for tunnelling through a molecular wire. *Phys. Rev. B* **57,** 1820–1823 (1998).

80. Tour, J. M., Kozaki M. & Seminario, J. M. Molecular scale electronics: a synthetic/computational approach to digital computing. *J. Am. Chem. Soc.* **120,** 8486–8493 (1998).

81. Sugiura, K. I., Tanaka, H., Matsumoto, T., Kawai, T. & Sakata, Y. A mandala-patterned bandanna-shaped porphyrin oligomer, $C_{1244}H_{1350}N_{84}Ni_{20}O_{88}$, having a unique size and geometry. *Chem. Lett.* 1193–1194 (1999).

82. Wada, Y. Atom electronics: a proposal of atom/molecule switching devices. *Ann. NY Acad. Sci.* **852,** 257–276 (1998).

83. Menon, M. & Srivastava, D. Carbon nanotube "T-junctions": nanoscale metal-semiconductor-metal contact devices. *Phys. Rev. Lett.* **79,** 4453–4456 (1997).

84. Stipe, B. C., Rezaei, M. A. & Ho, W. Inducing and viewing the rotation motion of a single molecule. *Science* **279,** 1907–1909 (1998).

85. Tans, S. J., Devoret, M. H., Groeneveld, R. J. A. & Dekker, C. Electron–electron correlations in carbon nanotubes. *Nature* **394,** 761–764 (1998).

86. Guo, L., Krauss, P. R. & Chou, S. Y. Nanoscale silicon field effect transistors fabricated using imprint lithography. *Appl. Phys. Lett.* **71,** 1881–1883 (1997).

87. Lüthi, R. *et al.* Parallel nanodevice fabrication using a combination of shadow mask and scanning probe methods. *Appl. Phys. Lett.* **75,** 1314–1316 (1999).

88. Kratschmer, E. *et al.* An electron-beam microcolumn with improved resolution beam current and stability. *J. Vac. Sci. Technol. B* **13,** 2498–2503 (1995).

89. Lefebvre, J., Lynch, J. F., Llaguno, M., Radosavljevic, M. & Johnson, A. T. Single-wall carbon nanotube circuits assembled with an atomic force microscope. *Appl. Phys. Lett.* **75,** 3014–3016 (1999).

90. Allara, D. L. *et al.* Evolution of strategies for self-assembly and hook up of molecule-based devices. *Ann. NY Acad. Sci.* **852,** 349–370 (1998).

91. Gerdes, S., Ondarcuhu, T., Cholet, S. & Joachim, C. Combing a carbon nanotube on a flat metal-insulator-metal nanojunction. *Europhys. Lett.* **48,** 292–298 (1999).

92. M. Handschuh, M., Nettesheim, S. & Zenobi, R. *Appl. Surf. Sci.* **137,** 125–135 (1999).

93. Philp, D. & Stoddart, J. F. Self-assembly in natural and unnatural systems. *Angew. Chem. Int. Edn Engl.* **35,** 1154–1196 (1996).

94. Drain, C. M. & Lehn, J. M. Self-assembly of square multiporphyrin arrays by metal ion coordination. *J. Chem. Soc. Chem. Commun.* 2313–2315 (1994).

95. Gimzewski, J. K. & Joachim, C. Nanoscale science of single molecules using local probes. *Science* **283,** 1683–1688 (1999).

96. Yazdani, A., Eigler, D. M. & Lang, N. D. Off-resonance conduction through atomic wires. *Science* **272,** 1912–1924 (1996).

97. Fischer, P. B. & Chou, S. Y. 10 nm electron beam lithography and sub-50 nm overlay using a modified scanning electron microscope. *Appl. Phys. Lett.* **62,** 2989–2991 (1993).

98. Bezradyin, A. & Dekker, C. Nanofabrication of electrodes with sub-5nm spacing for transport experiments on single molecules and metal clusters. *J. Vac. Sci. Technol. A* **15,** 793–799 (1997).

99. Morpurgo, A. F., Marcus, C. M. & Robinson, D. B. Controlled fabrication of metallic electrodes with atomic separations. *Appl. Phys. Lett.* **74,** 2084–2086 (1999).

100. Dietz, T. M., Stallman, B. J., Kwan, W. S. V., Penneau, J. F. & Miller, L. L. Soluble oligoimide molecular lines which have persistent poly(anion radicals) and poly(dianions). *J. Chem. Soc. Chem. Commun.* 367–369 (1990).

101. Kwan, W. S. V., Atanasoska, L. & Miller, L. L. Oligoimide monolayers covalently attached to gold. *Langmuir* **7,** 1419–1425 (1991).

102. Schumm, J. S., Pearson, D. L. & Tour, J. M. Iterative divergent/convergent doubling approach to linear conjugated oligomers. A rapid route potential molecular wire. *Macromolecules* **27,** 2348–2350 (1994).

103. Schumm, J. S., Pearson, D. L. & Tour, J. M. Iterative divergent/convergent doubling approach to linear conjugated oligomers. A rapid route to a 128 Å long potential molecular wire. *Angew. Chem. Int. Edn Engl.* **33,** 1360–1363 (1994).

104. Huang, S. & Tour, J. M. Rapid solid-phase synthesis of conjugated homo-oligomers and (AB) alternating block co-oligomers of precise length and constitution. *J. Org. Chem.* **64,** 8898–8906 (1999).

105. Kumar, A. & Whitesides, G. M. Features of gold having micrometer to centimeter dimensions can be formed through a combination of stamping with an elastomeric stamp and an alkanethiol 'ink' followed by chemical etching. *Appl. Phys. Lett.* **63,** 2002–2004 (1993).

106. Kumar, A., Biebuyck, H. A. & Whitesides, G. M. Patterning SAMs: Applications in materials science. *Langmuir* **10,** 1498–1511 (1994).